Journal of Computational Physics **164,** 354–376 (2000)
doi:10.1006/jcph.2000.6601, available online at http://www.idealibrary.com on IDEAL®

Reduction of Chemical Kinetics in Air Pollution Modeling

Bruno Sportisse and Rafik Djouad

Centre d'Enseignement et de Recherche Eau, Ville, Environnement, Ecole Nationale des Ponts et Chaussées (ENPC-CEREVE), rue Blaise Pascal, 77455 Champs sur Marne, France
E-mail: sportiss@cereve.enpc.fr, djouad@cereve.enpc.fr

Received November 30, 1999; revised June 6, 2000

We investigate in this article the use of reduction techniques in air pollution modeling. The reduction of chemical kinetics is performed on the basis of a timescale analysis and of lumping. Lumping techniques are widely used in air pollution modeling and consist of replacing some *pure* chemical species by linear combinations of species. We focus here on the theoretical justification of such techniques. We propose an algorithm in order to build up lumped species in a systematic way. An application to three kinetic schemes coupled with diffusion is presented in a monodimensional case. This justifies the way we couple a reduced kinetic scheme with other processes.

Key Words: air pollution modeling; tropospheric ozone; lumping techniques; reduction of chemical kinetics; numerical algorithms.

INTRODUCTION

Air pollution models describe the time and space evolution of some given chemical species in the troposphere [28]. They take into account many phenomena such as chemical kinetics, diffusion driven by turbulence, and advection by the wind field. Both the gas phase and the aqueous phase are eventually studied.

The numerical simulation of such models is particularly difficult [25, 38, 44]. The characteristic timescales of the system (that is, the eigenvalues of the associated Jacobian matrix) range indeed from very low values to high ones. This induces the well-known stiffness of such systems and leads to the use of specific tailored solvers for the time-integration (implicit solvers rather than explicit ones). We refer for instance to [9, 24, 27, 32, 37] for benchmarks and for the appropriate numerical schemes. The time integration of chemical kinetics remains, however, particularly time consuming.

An alternative approach amounts to reducing the system by eliminating the fast timescales [29]. Many methods have already been proposed [10, 16, 22, 26, 29] mainly for combustion processes. High-order methods can be found in [20, 34].

0021-9991/00 $35.00

We investigate in this article the building of reduced models for chemical kinetics and the coupling with other processes such as diffusion. The basis of our method is the use of lumped species.

Lumping techniques have already been widely used in air pollution modeling [11, 12]. The basic idea is to replace some fast species (species which take part in fast chemical processes) by linear combinations of fast species in the model. For instance, the most famous lumped scheme is associated with Chapman's cycle of tropospheric ozone,

$$\mathrm{O} + \mathrm{O}_2 \xrightarrow{1} \mathrm{O}_3, \quad \mathrm{NO}_2 + h\nu \xrightarrow{2} \mathrm{NO} + \mathrm{O}, \quad \mathrm{NO} + \mathrm{O}_3 \xrightarrow{3} \mathrm{NO}_2 + \mathrm{O}_2, \tag{1}$$

where the reaction 2 is photolytic ($h\nu$ denotes a photon). Many authors (following [12]) have proposed to replace the species NO_2 and O_3 respectively with the following lumped species:

$$\mathrm{NO}_x = \mathrm{NO} + \mathrm{NO}_2, \quad \mathrm{O}_x = \mathrm{NO}_2 + \mathrm{O}_3 + \mathrm{O}. \tag{2}$$

The reason usually invoked is the danger of numerical instability [12] and the search for mass conservation of some groups of atoms (here NO and O_2). The lumped species are, however, usually proposed without any further justification.

The aim of this article is to present a theoretical framework for such techniques and to propose some algorithms to build the underlying reduced model in an appropriate way. The "fast" numerical simulation of such reduced models needs either specific solvers we do not investigate here or the use of preprocessed tabulations.

We present briefly in the first section some general results concerning reduction and lumping. The key point is that the reduced system associated with chemical kinetics (OD case) can thereafter be used for the coupling with slow processes such as diffusion, emissions, and dry deposition. The use of lumped species is an alternative to the study of linearized systems, which is the kernel of the algorithms CSP [17] and ILDM [22]. The theoretical aspects can be found elsewhere for the case of ordinary differential equations [29] and for the extension to partial differential equations [31].

We present in the second section an algorithm for determining the lumped scheme in a systematic way. This is highly linked with an appropriate partitioning of species and reactions. The study of the eigenvalues of the Jacobian matrix provides a way for validating *a priori* such a partitioning.

In the third section we apply the previous algorithms to three atmospheric kinetic schemes in a monodimensional model including diffusion, emissions, and dry deposition.

1. REDUCING AND LUMPING TECHNIQUES

1.1. Slow–Fast Systems

Chemical kinetics can be characterized by the wide range of timescales: some reactions occur very quickly (fast dynamics), while others ones associated with large timescales (slow dynamics). This can be mathematically described by the singular perturbation theory [33]. The main feature is that all the trajectories in the phase space of concentrations converge to a unique curve after a fast transient phase, whatever the initial conditions. The evolution can thereafter be approximated by a slow motion along this low-dimensional manifold.

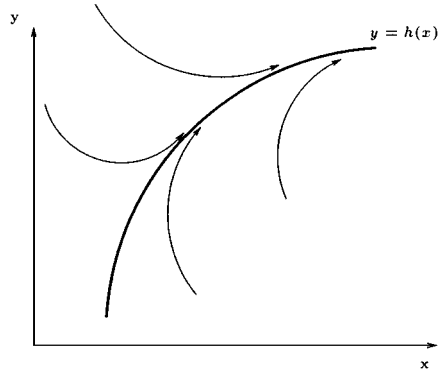

FIG. 1. Dynamical behaviour of chemical kinetics.

Let (x, y) be the set of concentrations, x and y being two subsets of concentrations. We have plotted in Fig. 1 such a behaviour by assuming that the low-dimensional manifold may be defined by the algebraic constraint $y = h(x)$. Reduction procedures are the search for the simplified model onto this manifold. The classical tool which is usually invoked is the so-called Tikhonov theorem [33].

THEOREM 1.1. *Let us consider the evolution system*

$$\frac{dx}{dt} = f_0(x, y) + \varepsilon f_1(x, y), \quad \varepsilon \frac{dy}{dt} = g_0(x, y) + \varepsilon g_1(x, y), \tag{3}$$

with $x \in \mathbf{R}^{n-p}$ *and* $y \in \mathbf{R}^p$ *subject to the initial conditions* $x(0) = x_0$ *and* $y(0) = y_0$. ε *is a small positive parameter describing the ratio of fast timescales on slow ones.*

For $t > 0$ *the initial model* (3) *can be approximated up to first-order in* ε *by the so-called reduced model,*

$$\frac{dx}{dt} = f_0(x, y) + \varepsilon f_1(x, y), \quad 0 = g_0(x, y), \tag{4}$$

where $0 = g_0(x, y)$ *defines* (*under some classical assumptions we do not precise here*) *a function* $y = h(x)$. *The initial conditions associated with* (4) *are the asymptotic points of the so-called inner layer*: $x(0) = x_0$ *and* $y(0) = h(x_0)$.

The equation describing the low-dimensional model can then be easily found by applying the well-known quasi-steady state assumption (QSSA) for species y, that is, by replacing the differential equation for y with the algebraic constraint $g_0(x, y) = 0$.

Systems arising in practice do not have, of course, the nice form (3). The key point for applying such techniques is then to find an appropriate partitioning in slow (x) and fast (y) species. We will now explain this point further in the next sections first by taking into account only chemical kinetics and then by coupling it with other processes supposed to be slow.

1.2. 0*D* Case

1.2.1. *Theory*

We assume here that all species can be viewed as fast ones in a first approach and we illustrate in this section the difficulties induced by a brute-force use of theorem 1.1. Let us

consider a dynamical system written under the general form

$$\varepsilon \frac{dx}{dt} = Mg_0(x, y) + \varepsilon f_1(x, y), \quad \varepsilon \frac{dy}{dt} = g_0(x, y) + \varepsilon g_1(x, y), \tag{5}$$

where $x \in \mathbf{R}^{n-p}$ and $y \in \mathbf{R}^p$ stand for two subsets of chemical concentrations, and ε is as before a small positive parameter defined as the ratio of timescales. The key point is that x and y are concerned by fast dynamics given respectively by Mg_0 and g_0. M is a matrix of dimension $(n - p) \times p$ describing the fast coupling between x and y. For more clarity, we have assumed that the fast dynamics are linearly coupled through M. Such an assumption is actually met in practice for chemical kinetics due to the stoichiometric form of the chemical production term (see [8, 36]). This is somehow an assumption which is useful for clarity but not necessary for the kernel of the theory.

The key point in order to reduce this sytem is to eliminate the fast coupling between species. One possible procedure is to lump species by replacing x with

$$u = x - My. \tag{6}$$

In the new basis (u, y), we have easily

$$\frac{du}{dt} = f_1(.) - Mg_1(.), \quad \varepsilon \frac{dy}{dt} = g_0(.) + \varepsilon g_1(.), \tag{7}$$

where the functions $f_1(.)$, $g_1(.)$, and $g_0(.)$ are computed at $(u + My, y)$. u appears now as a slow variable and a QSSA procedure can be applied to y in this basis. This leads to the algebraic constraint

$$g_0(u + My, y) = 0. \tag{8}$$

This defines y as a function of u under some classical hypothesis, mainly that the following matrix is nonsingular along the constraint (8)

$$\frac{\partial g_0}{\partial y} + \frac{\partial g_0}{\partial x} M. \tag{9}$$

Such an assumption is indeed necessary and sufficient for justifying the existence of a reduced model with p algebraic constraints (see [8, 29], for instance). Let us notice that (8) is exactly $g_0(x, y) = 0$ with $u = x - My$.

We now go back to the initial basis and we find

$$\frac{dx}{dt} = \left(I + M \left(\frac{\partial g_0}{\partial y} + \frac{\partial g_0}{\partial x} M \right)^{-1} \frac{\partial g_0}{\partial x} \right) (f_1(.) - Mg_1(.)), \quad g_0(x, y) = 0. \tag{10}$$

We do not use (10) in our numerical tests, because this would require the computation of a rather complicated local projection matrix. Another way we advocate is to solve the reduced system in the lumped basis, that is, (7).

1.2.2. *Applications to Air Pollution Modeling*

We first apply this framework to gas-phase air pollution models in order to justify the use of the so-called "lumped species" [12].

We study a kinetic scheme whose fast part is given by the so-called Chapman cycle (1):

$$\mathrm{O} + \mathrm{O}_2 \xrightarrow{1} \mathrm{O}_3, \quad \mathrm{NO}_2 + h\nu \xrightarrow{2} \mathrm{NO} + \mathrm{O}, \quad \mathrm{NO} + \mathrm{O}_3 \xrightarrow{3} \mathrm{NO}_2 + \mathrm{O}_2. \tag{11}$$

We suppose therefore that reactions 1, 2, and 3 are fast and that all the other reactions in the kinetic scheme are slow. The other species are associated with a vector of concentration c and are slow species. We write, for instance,

$$x = \begin{bmatrix} \mathrm{NO} \\ \mathrm{O}_3 \end{bmatrix}, \quad y = \begin{bmatrix} \mathrm{NO}_2 \\ \mathrm{O} \end{bmatrix}, \tag{12}$$

where NO stands, for instance, for the symbol of the chemical species and for the concentration as well. The ODE giving the time evolution of species is

$$\frac{dc}{dt} = a(.), \quad \varepsilon \frac{dx}{dt} = f_0(x, y) + \varepsilon f(.), \quad \varepsilon \frac{dy}{dt} = g_0(x, y) + \varepsilon g_1(.), \tag{13}$$

where $a(.)$, $f_1(.)$, and $g_1(.)$ stand for the slow reaction terms and are computed at (c, x, y). The fast reaction terms are

$$f_0(x, y) = \begin{bmatrix} -\omega_2 + \omega_3 \\ \omega_1 - \omega_3 \end{bmatrix}, \quad g_0(x, y) = \begin{bmatrix} \omega_2 - \omega_3 \\ \omega_2 - \omega_1 \end{bmatrix}, \tag{14}$$

where $\frac{\omega_i}{\varepsilon}$ stands for the fast reaction rate associated with the reaction i and is given by the law of mass action. We recover easily the former formalism by defining M as

$$M = \begin{bmatrix} -1 & 0 \\ -1 & -1 \end{bmatrix}. \tag{15}$$

The lumping we have to use is then

$$u = x - My = \begin{bmatrix} \mathrm{NO} + \mathrm{NO}_2 \\ \mathrm{O}_3 + \mathrm{NO}_2 + \mathrm{O} \end{bmatrix}, \tag{16}$$

which is exactly the classical lumped scheme.

Remark. Lumped species may be defined in another way in atmospheric context. Another purpose is to lump slow species (typically volatile organic compounds) according to structural chemical relations. A simple example is provided by the following kinetic scheme:

$$X + Y_1 \xrightarrow{k} P + P_1, \quad X + Y_2 \xrightarrow{k} P + P_2. \tag{17}$$

We suppose that the law of mass action may be applied. k is the kinetic constant for both reactions.

If we are only interested in the product P but not in the by-products P_1 and P_2, we can define the lumped species $Y = Y_1 + Y_2$. The evolution of the concentrations of X, Y, and P is now (with obvious notations)

$$\frac{dx}{dt} = \frac{dy}{dt} = -kxy, \quad \frac{dp}{dt} = kxy. \tag{18}$$

The drawback is that we are not able to follow the evolution of Y_1 and Y_2.

This approach has nothing to do with a dynamical behaviour and we do not focus on this approach. We refer, for instance, to [3, 23] for a deeper understanding. Let us notice that such a strategy is usually known as "lumping" in the sense of [18, 19, 41, 40].

1.3. Coupling with Slow Processes

1.3.1. *Theory*

We consider now the coupling of a given kinetic scheme with a slow process T. T may be, for instance, a diffusion-advection term (PDE before spatial discretization) or an ODE term obtained by applying the method of lines. We refer to [31] for more details.

We keep the same form as before for the chemical production and loss term. T_x and T_y are the components of T for x and y. The evolution of the vector of concentrations z is now given by

$$\varepsilon \frac{dz}{dt} = \chi(z) + \varepsilon T(z), \tag{19}$$

where

$$z = \begin{bmatrix} x \\ y \end{bmatrix}, \quad \chi(z) = \begin{bmatrix} Mg_0(z) + \varepsilon f_1(z) \\ g_0(z) + \varepsilon g_1(z) \end{bmatrix}, \quad T(z) = \begin{bmatrix} T_x(z) \\ T_y(z) \end{bmatrix}. \tag{20}$$

The simplest way to proceed is to put the system into the basis of lumped species under the form

$$\frac{du}{dt} = f_1(.) + T_x(.) - M(g_1(.) + T_y(.)), \quad \varepsilon \frac{dy}{dt} = g_0(.) + \varepsilon(g_1(.) + T_y(.)), \tag{21}$$

where all functions are computed at $(u + My, y)$. This leads easily to the reduced system

$$\frac{du}{dt} = f_1(.) - Mg_1(.) + T_x(.) - MT_y(.), \quad 0 = g_0(u + My, y). \tag{22}$$

The key point is that the algebraic constraint is a local one $y = y(u)$ and is **the same one as in the OD case**. Let us notice that the term T has been modified through the lumping, because we have also to compute $T_x(u + My, y) - MT_y(u + My, y)$.

1.3.2. *Applications to Air Pollution Modeling*

We discuss now some simplifications that may occur in the case of air pollution modeling. Let us consider the case of a monodimensional reaction–diffusion PDE with Neumann boundary conditions describing the time evolution and the vertical profile of some trace gases. The vector of concentrations is $z \in \mathbf{R}^n$. We neglect the horizontal advection by the

wind field. Let us notice that this is quite realistic for some air pollution episodes. For the species i we have, for instance,

$$\frac{\partial z_i}{\partial t} = \mathrm{div}(k\nabla z_i) + \chi_i(z) \tag{23}$$

subject to the following boundary conditions:

- At the ground, $k\frac{\partial z_i}{\partial \nu} = -E_i(t) + v_{\mathrm{dep}_i} z_i$.
- At the top of the monodimensional column, $k\frac{\partial z_i}{\partial \nu} = 0$.

χ_i is the chemical production and loss term for species i. We take a *scalar* turbulent diffusion $T = k\Delta$, where k is the vertical turbulent diffusivity (the same value for all species) and Δ stands for the Laplacian operator. Dry deposition and emissions are added as boundary conditions at the ground where E is the emission vector and v_{dep} is the vector of dry deposition velocities. $\frac{\partial}{\partial \nu}$ stands for the normal derivative.

In the same way as before we will partition the vectors E and v_{dep} according to

$$E = \begin{bmatrix} E_x \\ E_y \end{bmatrix}, \quad v_{\mathrm{dep}} = \begin{bmatrix} v_{\mathrm{dep}_x} \\ v_{\mathrm{dep}_y} \end{bmatrix}. \tag{24}$$

Let us investigate the effect of lumping. For the diffusive part $T(z) = k\Delta z$ we have easily

$$T_x(u + My, y) = k\Delta u + kM\Delta y, \quad MT_y(u + My, y) = kM\Delta y \tag{25}$$

and then

$$T_x(u + My, y) - MT_y(u + My, y) = k\Delta u. \tag{26}$$

This is exactly $T_x(u, y)$ and we do not have to lump the diffusive part. On the contrary, the terms issued from boundary conditions have to be lumped since

$$(T_x - MT_y)(u + My, y) = -(E_x - ME_y) + v_{\mathrm{dep}_x} u + \left(v_{\mathrm{dep}_x} M - M v_{\mathrm{dep}_y}\right) y, \tag{27}$$

where $T(z) = k\frac{\partial z}{\partial \nu}$ stands now for the boundary operator.

The reduced model is then in the lumped basis

$$\frac{\partial u}{\partial t} = k\Delta u + f_1(u + My, y) - Mg_1(u + My, y), \quad 0 = g_0(u + My, y) \tag{28}$$

and subject to the following boundary conditions:

- At the ground, $k\frac{\partial u}{\partial \nu} = -(E_x - ME_y) + v_{\mathrm{dep}_x} u + (v_{\mathrm{dep}_x} M - M v_{\mathrm{dep}_y}) y$.
- At the top of the monodimensional column, $k\frac{\partial u}{\partial \nu} = 0$.

We have therefore to deal carefully with boundary conditions.

We will now propose an algorithm in order to build lumped species for any kinetic schemes and apply it to some monodimensional test cases arising in air pollution modeling.

2. AN ALGORITHM FOR BUILDING LUMPED SCHEMES

The main objective of this section is to describe an algorithm for the automatic computation of reduced models. This is done by selecting the fast species concerned with the QSSA approximation and by searching for the lumped species.

2.1. Partitioning Slow and Fast Dynamics

Let us consider a kinetic scheme describing the interaction of n species through n_r chemical reactions. Let z be the vector of concentrations. The time evolution due to chemical production and loss is then

$$\frac{dz}{dt} = S\omega, \quad J = S\left(\frac{\partial \omega}{\partial z}\right), \tag{29}$$

where S is the constant stoichiometric matrix $n \times n_r$, $\omega \in \mathbf{R}^{n_r}$ is the vector of reaction rates, and J is the Jacobian matrix of the system. We are going to partition J into the sum of a fast and a slow part as

$$J = J_0 + J_1, \quad J_0 = S_0\left(\frac{\partial \omega}{\partial z}\right), \quad J_1 = S_1\left(\frac{\partial \omega}{\partial z}\right), \tag{30}$$

where S_0 and S_1 are respectively the fast and slow stoichiometric matrices and $S = S_0 + S_1$. Provided that the rank of the fast part of the Jacobian matrix J_0 is equal to the number of fast species (eventually after a lumping of species if necessary), the algebraic constraint $S_0\omega(z) = 0$ can be directly solved in order to determine the fast species as a function of the slow ones.

We describe hereafter the filtering techniques we use to obtain a well-partitioned system. The key point is that we partition the stoichiometric matrix.

2.1.1. *Fast Species*

Many criteria can be used in order to detect fast species. Partitioning with respect to the magnitude of diagonal elements of the Jacobian matrix is usually proposed (see, for instance, [35, 43]). This can lead, however, to a wrong partitioning due to the nondominance of the diagonal. Let us recall that such a procedure is often used for hybrid ODE solvers [9, 32, 43].

The second criterion consists of the evaluation of the scaled ratio

$$I^i_{\mathrm{QSSA}} = \frac{|P_i - C_i|}{P_i + C_i} \tag{31}$$

for each species i. P_i and C_i are the production and loss terms of species i whose evolution is written under the form

$$\frac{dz_i}{dt} = P_i - C_i. \tag{32}$$

If I^i_{QSSA} is less than a prescribed small parameter ($\varepsilon \sim 10^{-2}$), then the species i is considered a fast one and the QSSA approximation ($P_i - C_i \sim 0$) can be applied. Otherwise it is considered slow and the corresponding fast stoichiometric coefficients are set equal to zero.

We advocate such a criterion because it is deeply linked with the dynamical behaviour of the system, while the lifetime may be constant during the whole time integration for linear systems.

2.1.2. *Fast Reactions*

To select the fast reactions associated with species i, many criteria have already been proposed. We can perform a scaling of the vector of reaction rates ω (as in [36]). Turanyi *et al*. have proposed the following ratio [35] for the reaction j,

$$\delta_j = \frac{\frac{1}{\omega_j}\frac{d\omega_j}{dt}}{J^r_{jj}}, \tag{33}$$

where J^r_{jj} is the diagonal element of the Jacobian matrix J^r associated with the linearized system for the time evolution of reaction rates,

$$\frac{d\omega}{dt} = J^r\omega, \quad J^r = \left(\frac{\partial\omega}{\partial z}\right)S, \tag{34}$$

and δ_j is the ratio of the transition time (inner layer) to the characteristic time of the reaction. As a consequence of classical results in linear algebra [42] the matrices J and J^r have the same eigenvalues except eventually 0 (compare Eqs. (29) and (34)). That is, J^r gives a good description of the slow–fast structure of the species system.

Such criteria, however, do not give a suitable partitioning. The simplest way to verify this is a computation of the resulting fast Jacobian eigenvalues, which are not exactly the large negative eigenvalues of the Jacobian matrix J (see next section). The reason is that such procedures are linked with an *a priori* partitioning of the reactions, independent of the coupling with species.

Let us consider a *fast* species i whose equation is in the form

$$\frac{dz_i}{dt} = \sum_{j=1}^{n_r} S_{ij}\omega_j. \tag{35}$$

To recover a partitioning among a linear combination of large positive terms (eventually balanced) and of small positive terms, we compute for every reaction j the relative contribution,

$$\gamma_j^i = \frac{|S_{ij}|\omega_j}{\sum_{k=1}^{n_r}|S_{ik}|\omega_k}. \tag{36}$$

The reaction j is said to have a slow contribution for the evolution of species i if γ_j^i is less than a prescribed small parameter ($\varepsilon \sim 10^{-2}$). Let us notice that such a criterion has already been proposed in [15, 17] for other purposes.

To conclude, we compute the fast stoichiometric matrix S_0 in the following way:

- For a slow species i, we set $(S_0)_{ij} = 0$ for all j.
- For a fast species i, we set $(S_0)_{ij} = 0$ if $\gamma_j^i < \varepsilon$; otherwise $(S_0)_{ij} = S_{ij}$.

2.2. Lumped Species

If the number of fast species is greater than the rank of the fast Jacobian matrix J_0, then a lumping of species is necessary for solving the QSSA algebraic constraints. Otherwise,

the resulting system is underdetermined. We have then to define a new set of slow species, which for the contribution of fast reactions is zero. In practice we have to search for a basis of the left kernel of the matrix S_0. The choice of this basis is completely free and does not have any impact on the accuracy of the reduced model.

The algorithm we propose is then the following one:

1. Select fast species with the use of (31).
2. Select fast reactions for fast species with the use of (36).
3. Compute S_0.
4. Compute a basis $(v_1, \ldots, v_r)$ of the left kernel of S_0, where $r = n - \text{rank}(S_0)$. The vectors v_i are in $\mathbf{R}^n$ and satisfy $v_i \cdot S_0 = 0$.
5. Define r lumped species as follows for $i = 1, \ldots, r$,

$$u_i = v_i \cdot z, \tag{37}$$

where $\cdot$ denotes the usual scalar product of $\mathbf{R}^n$.

It is easy to check that u_i is not related to fast dynamics since

$$\frac{du_i}{dt} = v_i \cdot \frac{dz}{dt} = v_i \cdot S_1 \omega. \tag{38}$$

The key point, of course, is that the left kernel of S_0 is exactly the left kernel of $J_0 = S_0(\frac{\partial \omega}{\partial z})$. Such a result can be mathematically proved under some axiomatic conditions for chemical kinetics (see [29, 39]). It is unfortunately impossible to give a proof for any kinetic schemes such as those arising in atmospheric chemistry, since the reactions in general are not elementary ones (that is, they do not necessary describe collisions between molecules). Let us point out that the partitioning is *a priori* a local one. Our numerical tests confirm, however, that the partitioning is constant over transient phases related to changes in photolytic chemistry (that is, at sunrise and sunset). This is a particular feature of atmospheric chemistry in which temperature does not play a crucial role, in contrast to combustion. This confirms that we can search for a global reduced model as given by a singular perturbation form rather than by a local reduced model as given by methods such as ILDM and CSP.

2.3. Validation

We have applied the previous algorithm to three different kinetic schemes:

1. The so-called "Jacob scheme."
2. The so-called "Kim–Cho scheme" [14].
3. The so-called "Ozone 16 scheme" [2].

The main characteristics of these models can be found in Table I and in the Appendix. Let us note that they only include gas-phase chemistry. We refer to the references for a more detailed description of the kinetic schemes.

The accuracy of the reduced models depends on the validity of the partitioning. We perform *a priori* a validation of the partitioning by the following method. We compare the strictly negative eigenvalues of the fast part J_0 and the most negative eigenvalues of the Jacobian J. The other eigenvalues of J_0 are 0 and are associated with the less negative eigenvalues of J.

Let us point out that we do not have to compute the Jacobian matrix for applying our algorithm, in contrast to techniques such as ILDM and CSP, which are based on the study of the linearized system (which is much more appropriate for systems with a local definition of the reduced system, as those arising in combustion). In this section, we compute the Jacobian matrix for checking the validity of the partitioning.

The key point is that the large negative eigenvalues of J must be preserved (according to [4]). Let r be the number of large negative eigenvalues of J. Let $\{\lambda_i(t_n)\}_i$ and $\{\lambda_{fi}(t_n)\}_i$ be the set of eigenvalues (in increasing order) respectively for J_0 and J at time $t_n = n\Delta t$. The average relative error err has been computed in Table II through

$$\text{err} = \frac{1}{Nr} \sum_{n=1}^{N} \sum_{i=1}^{r} \left(\frac{|\lambda_i(t_n) - \lambda_{fi}(t_n)|}{\lambda_{fi(t_n)}} \right), \tag{39}$$

where N is the number of time steps. See the next section for the values of Δt and N.

The results for the three kinetic schemes can be found in Tables III, IV, and V. We have only plotted the results at a given time ($t = 0$), but the same holds for any time (with different values due to the nonlinearity of the system).

The resulting lumping is given in Table VI. We have given only lumped species defined by linear combinations of fast species and we have excluded pure slow species. We recover in these examples the usual lumped species up to some minor algebraic manipulations [11, 12]. The package LSODE [13] has been used to perform the integration. Let us recall that p is the number of QSSA species (given by the QSSA index) and rank(J_0) is the number of algebraic constraints to be used. The number of such lumped species is $p -$ rank(J_0).

Remark [Comparison with the study of linearized systems]. Let us notice that we compute the left kernel of the fast part of the Jacobian matrix J_0, that is, the left kernel of S_0. If the partitioning of dynamics is constant, this gives constant lumping vectors.

In contrast, methods based on the study of the Jacobian matrix, such as ILDM and CSP, compute left eigenvectors of J.

3. REDUCED MECHANISMS IN A MONODIMENSIONAL CASE

3.1. Strategy

We have performed some numerical tests with the previous algorithms:

1. We perform first a preprocessed computation in the OD case in order to derive a lumped scheme (u, y). This does not require computation of the Jacobian matrix.

2. We use this lumped scheme to solve the kinetic scheme in the 1D case. We use the differential-algebraic solver LIMEX [5, 6] to solve the reduced system given by Eq. (28) and thereafter we go back to the initial basis of species (x, y). As pointed out above we advocate this strategy in order to avoid the computation of complicated projection matrices.

To assess the accuracy of the reduced models we compute with LSODE [13] ($mf = 21$, Newton iterations) a time-accurate solution which is obtained through the method of lines and finite differences for the 1D case. This reference solution is defined by the original model. The reduced solution is computed with LIMEX. In both solvers the Jacobian matrices are computed with finite differences. As the units are molecules per cubic centimeter, we use

TABLE I
Kinetic Schemes

	Jacob scheme	Kim–Cho scheme	Ozone 16 scheme
Species	10	15	16
Reactions	9	21	12
Units	Molecules cm^{-3}	ppm	Molecules cm^{-3}

TABLE II
Mean Relative Error for Filtering (err)

Jacob scheme	Kim–Cho scheme	Ozone 16 scheme
6.2E-4	0.1E-2	4.2E-2

TABLE III
Eigenvalues for Jacob Scheme

λ_i	−18.34	−0.72	−4.9E-2	−2.42E-2	−4.0E-7
λ_{fi}	−18.34	−0.72	−4.89E-2	−2.42E-2	0

TABLE IV
Eigenvalues for Kim–Cho Scheme

λ_i	−20.88	−8.96	−3.74	−5.32E-2	−8.94E-3	−1.05E-3
λ_{fi}	−20.87	−8.95	−3.74	−5.32E-2	−8.91E-3	0

TABLE V
Eigenvalues for Ozone 16 Scheme

λ_i	−61665.37	−889.57	−25.07	−1.01	−0.54	−0.41	−1.57E-5
λ_{fi}	−61665.37	−832.51	−24.38	−1.00	−0.51	−0.44	0

TABLE VI
Generated Lumping

Scheme	p	rank (J_0)	Computed lumping
Kim–Cho	7	5	$\begin{cases} U_1 = -0.5\mathrm{NO} - \mathrm{NO_2} - 0.5\mathrm{O_3} \\ U_2 = 0.71\mathrm{NO} + \mathrm{NO_2} + 0.29\mathrm{O_3} \end{cases}$
Ozone 16	8	6	$\begin{cases} U_1 = -2\mathrm{NO} - 3\mathrm{NO_2} - \mathrm{O_3} - \mathrm{OD} \\ U_2 = -3.3\mathrm{NO} - 2.3\mathrm{NO_2} + \mathrm{O_3} + \mathrm{OD} \end{cases}$
Jacob	6	4	$\begin{cases} U_1 = \mathrm{NO} - \mathrm{NO_2} - 2\mathrm{O_3} \\ U_2 = -\mathrm{NO} + 2\mathrm{NO_2} + 3\mathrm{O_3} \end{cases}$

as control parameters atol = 1.0 and rtol = 1.E-5, whereas for ppm, we use atol = 1.E-7 and rtol = 1.E-5 instead. The initial conditions are modified to make the reduced model valid from the beginning of the computation by solving the exact model during the transient phase. This is of course not very interesting in a general application, but we focus here on the accuracy of reduced models.

We use the following norms to evaluate the relative errors:

- A spatial L_2 norm at a fixed timestep $t_n = n\Delta t$ for the species i,

$$r_i(n) = \sqrt{\sum_{m=1}^{m=M} \mathrm{err}_i(n,m)^2\, dx_m}, \tag{40}$$

where i, n, and m denote respectively the index for species (I species), timesteps (N timesteps of length $\Delta t = 900$ s), and grid cells (M grid cells). dx_m is the length of the m grid cell and err_i is the relative error for species i,

$$\mathrm{err}_i(n,m) = \frac{z_i^{\mathrm{ex}}(n,m) - z_i^{\mathrm{red}}(n,m)}{z_i^{\mathrm{ex}}(n,m) + \mathrm{atol}}, \tag{41}$$

where z^{ex} and z^{red} are respectively the exact and reduced solutions.

The L_1 average of these norms is

$$\langle r(n)\rangle = \frac{1}{I}\sum_{i=1}^{i=I} r_i(n). \tag{42}$$

- A spatial L_2 norm for the time integration on $[0, t_n]$:

$$gr_i(n) = \sqrt{\frac{1}{N}\sum_{m,k=1}^{m=M,k=n} \mathrm{err}_i(k,m)^2\, dx_m}. \tag{43}$$

The L_1 average of these norms is

$$\langle gr(n)\rangle = \frac{1}{I}\sum_{i=1}^{i=I} gr_i(n). \tag{44}$$

We compute the number of correct digits nd and ndg given by

$$r_i(n) = 10^{-nd(i,n)}, \quad gr_i(n) = 10^{-ndg(i,n)}, \quad \langle r(n)\rangle = 10^{-nd(n)}, \quad \langle gr(n)\rangle = 10^{-ndg(n)}. \tag{45}$$

All these numbers are computed at the end of the integration in the following sections ($n = N$).

Remark [CPU performance]. Let us point out once more that we do not investigate here the CPU performance of the reduced model, because we are interested in a simple computation of the reduced model and in the accurate coupling with transport. This would otherwise require either a specific low-order solver for the integration of the resulting

differential-algebraic system [7] or the preprocessed computation of the solution of the algebraic constraints (for instance, with some kind of polynomial expansion as in [21]).

This is confirmed by the following experiment: if we use LIMEX as an ODE solver for the exact unreduced model, we have minor differences (around 10%) in the same CPU time as is required for the reduced model. This is not surprising, because we have to solve in both cases algebraic constraints, given either by an implicit scheme or by the reducing process.

Remark [Reduction and splitting]. Splitting and reduction are deeply linked for such slow–fast systems. We refer to [30] for a deeper understanding. The key point is that using preprocessed tables of the reduced model in a splitting context could be quite hazardous because the diffusion step removes the variables far from the reduced model, making the tabulation poorly accurate.

3.2. Results

3.2.1. *Ozone 16 Scheme*

We have used three distinct sets of initial conditions, corresponding to three types of emissions (rural, urban, regional: respectively, CI_1, CI_2, and CI_3) to check that we can define the reduced model in a global way. We refer to [2] for more details.

We have first used the lumping I defined by omitting atomic oxygen OD in the lumping given in Table VI. The lumping with OD (lumping II) gives similar results. The results are shown for the first set of initial conditions in Table VII. Good accuracy is obtained as well for the second set of initial conditions with the use of lumping I: results are given in Table VII among brackets.

To illustrate the necessity of lumping the transport terms, we have tried to integrate a system without lumping the transport terms (for instance, in the case CI_3). In Table VIII the stars indicate the loss of any accuracy.

TABLE VII
Number of Correct Digits *nd*(*i*, *N*) and *ndg*(*i*, *N*)

	nd (I)	*ndg* (I)	*nd* (II)	*ndg* (II)
Air	5.54 (4.66)	5.57 (4.81)	5.54	5.57
O_2	5.78 (4.66)	5.69 (4.81)	5.78	5.69
CO_2	3.13 (2.80)	2.93 (2.82)	3.13	2.93
HNO_3	4.05 (3.43)	3.58 (3.44)	4.05	3.58
RH	3.73 (3.94)	3.71 (3.92)	3.73	3.71
CO	4.67 (4.19)	4.66 (4.36)	4.67	4.66
NO	2.34 (2.47)	2.39 (2.68)	2.34	2.39
NO_2	3.79 (3.00)	3.31 (2.95)	3.79	3.31
PAN	4.00 (2.52)	3.84 (2.62)	4.00	3.84
RCHO	4.69 (3.62)	4.66 (3.71)	4.69	4.66
O_3	3.17 (2.03)	2.34 (1.89)	3.17	2.34
OH	2.83 (2.83)	2.96 (2.83)	2.83	2.96
HO_2	2.57 (2.43)	2.77 (2.67)	2.57	2.77
RCO_3	3.09 (2.70)	3.11 (2.92)	3.09	3.11
RO_2	2.66 (2.49)	2.84 (2.73)	2.66	2.84
OD	3.75 (2.98)	3.31 (2.93)	3.75	3.31

Note. Lumpings I and II are used for Ozone 16 with the scenario CI_1. The values in parentheses are associated with the scenario CI_2.

TABLE VIII
Number of Correct Digits *nd*(*i*, *N*) and *ndg*(*i*, *N*)

	nd (I)	*ndg* (I)	*nd* (*)	*ndg* (*)
Air	5.19	5.31	5.09	5.24
O_2	5.19	5.33	5.19	5.27
CO_2	2.97	2.99	0.34	0.35
HNO_3	3.53	3.31	0.17	0.23
RH	3.53	3.39	2.28	2.20
CO	4.62	4.51	1.66	1.87
NO	3.15	2.63	0.04	0.04
NO_2	4.33	3.44	0.08	0.16
PAN	3.62	3.31	0.31	0.27
RCHO	4.78	4.87	1.36	1.55
O_3	2.53	1.98	0.16	*
OH	3.36	3.11	0.63	0.56
HO_2	2.65	2.58	*	*
RCO_3	3.28	3.36	*	*
RO_2	2.72	2.67	*	*
OD	4.22	3.45	0.08	0.16

Note. Scenario CI_3 with (I) and without (*) lumping the transport terms for Ozone 16.

Global results can be found in Table IX.

3.2.2. *Kim–Cho Scheme*

The same procedure has been applied to an inorganic kinetic scheme which has been derived from the works of Atkinson and Lloyds [14]. The lumping I performs in an excellent way, except for the species HONO (Table X). The study of the spatial profile of the error indicates that the error is mostly in the first cells (near the ground). The reason is probably the influence of the boundary conditions terms (emissions and dry deposition), which are not as slow as assumed in our analysis. The spatial profile of the QSSA ratio for species HONO confirms that the boundary conditions remove HONO from the center manifold (Fig. 2).

We have therefore computed the lumped scheme I in all the grid cells, except in the first grid cell where we have used the exact solution. Such a model (lumping III) improves the accuracy of the reduced solutions, which seems to be logical since a part of the exact scheme is used. To prove that the hypothesis of slow transport can induce low errors, we have tested another lumped scheme by replacing for fast species the local algebraic constraint we write

TABLE IX
Number of Correct Digits *nd*(*N*) and *ndg*(*N*) for Ozone 16

	N	*nd*	*ndg*
CI_1 (I)	24	3.06	2.77
CI_1 (II)	24	3.06	2.77
CI_2 (I)	24	2.72	2.46
CI_3 (I)	24	3.17	2.55
CI_3 (without lumping)	24	*	*

TABLE X
Number of Correct Digits *nd*(*i*, *N*) and *ndg*(*i*, *N*): Case Kim–Cho

	nd (I)	*ndg* (I)	*nd* (III)	*ndg* (III)	*nd* (IV)	*ndg* (IV)	*nd* (*)	*ndg* (*)
HNO_3	3.04	3.06	3.15	3.19	3.96	3.98	1.60	1.80
H_2O_2	5.48	5.50	4.19	4.14	4.19	4.14	5.52	5.51
NO	3.07	3.08	3.77	3.80	4.02	3.88	0.74	0.90
NO_2	3.11	3.17	3.98	4.07	4.01	3.91	1.14	1.31
O_3	3.11	3.11	3.94	3.93	3.89	3.82	1.07	1.21
OH	2.27	2.29	2.50	2.52	3.61	3.51	0.85	1.00
HONO	1.78	1.79	1.94	1.95	3.46	3.34	1.77	1.77
HO_2	2.34	2.36	2.52	2.54	3.82	3.74	0.59	0.73
HO_2NO_2	2.42	2.43	2.53	2.54	4.14	4.17	0.68	0.82
NO_3	3.03	3.09	3.66	3.78	4.30	4.10	0.80	0.93
N_2O_5	2.63	2.68	3.25	3.31	3.75	3.77	0.98	1.11
SO_2	4.93	5.11	4.88	4.69	4.67	4.61	3.34	3.62
H_2SO_4	2.99	3.06	3.15	3.21	3.88	3.94	1.41	1.63

formally under the form $\chi(c) = 0$ by the global algebraic constraint $\chi(c) + T(c) = 0$. This lumped scheme (lumping IV) gives the best results.

As before, the reduced model obtained without lumping the transport terms gives poor accuracy (Table X). Global results can be found in Table XI.

Remark [Night-time chemistry]. To prove the dependence of the reduced scheme on the photolysis, we have performed the same computation under night-time conditions. We have therefore cancelled all kinetic rates for photolytic reactions. The dynamical behaviour of the system is then drastically modified and a new lumping is obtained with our procedure:

$$NO_y = NO_3 + N_2O_5, \quad NO_z = NO_3 - NO_2. \tag{46}$$

We use then the QSSA for species OH, HO_2, HO_2NO_2, and NO_3 while N_2O_5 is replaced with NO_y. This gives an explanation of the use of such a lumped scheme by some atmospheric chemists.

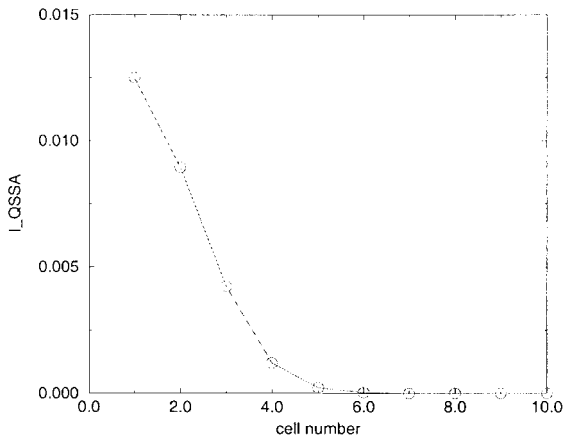

FIG. 2. I_{QSSA} for species HONO after 20 iterations.

TABLE XI

Number of Correct Digits *nd*(*N*) and *ndg*(*N*): Case Kim–Cho

	N	*nd*	*ndg*
Lumping I	20	2.60	2.33
Lumping III	20	2.81	2.50
Lumping IV	20	3.95	3.76
Without lumping	20	1.06	1.07

TABLE XII

Number of Correct Digits *nd*(*i, N*) and *ndg*(*i, N*): Case Jacob

	nd (I)	*ndg* (I)	*nd* (III)	*ndg* (III)	*nd* (IV)	*ndg* (IV)
ROOH	2.83	2.50	2.81	2.50	2.86	2.48
HNO_3	3.12	2.02	3.08	2.03	2.92	2.00
H_2O_2	3.81	3.04	3.95	3.04	3.78	2.98
RH	3.38	2.47	3.35	2.47	3.29	2.37
NO	2.14	2.02	2.72	2.31	3.10	2.30
NO_2	2.43	2.15	3.24	2.22	2.94	2.10
O_3	2.29	2.40	3.18	2.76	2.72	2.60
OH	2.02	1.75	1.74	1.78	1.77	1.57
RO_2	2.51	1.79	1.83	1.77	1.79	1.58
HO_2	2.48	1.79	1.83	1.77	1.80	1.58

TABLE XIII

Number of Correct Digits *nd*(*i, N*) and *ndg*(*i, N*): Case Jacob without Lumping

	nd (a)	*ndg* (a)	*nd* (b)	*ndg* (b)
ROOH	0.65	0.79	0.04	0.33
HNO_3	0.06	0.13	0.85	1.07
H_2O_2	0.75	0.93	2.04	2.44
RH	0.45	0.68	1.47	1.89
NO	0.28	0.48	0.19	0.36
NO_2	0.25	0.46	0.33	0.52
O_3	0.72	0.91	0.19	0.49
OH	*	*	*	*
RO_2	*	*	*	*
HO_2	*	*	*	*

TABLE XIV

Number of Correct Digits *nd*(*N*) and *ndg*(*N*): Case Jacob

	N	*nd*	*ndg*
Lumping I	24	2.46	1.98
Lumping III	24	2.27	2.00
Lumping IV	24	2.25	1.82
Without lumping (a)	24	*	*
Without lumping (b)	24	*	*

3.2.3. *Jacob Scheme*

This kinetic scheme is much more interesting because the photolytic dependence has been conserved, which leads to a nonautonomous system. However, this does not change the lumped species for day-time simulations.

We have used lumping I once more. Lumping techniques III (exact solution in the first grid cell) and IV (global algebraic constraint) give less accurate results here. This is in contradiction with the previous computations performed for the Kim–Cho case and could indicate that the assumption of slow transport gives here the best accuracy of the reduced scheme (Table XII).

The procedures without lumping give wrong results as before (Table XIII). We have tested here two such procedures to prove that it does not depend on the number of QSSA species but on the lack of lumping (Table XIV):

- In the first procedure (a), four species (OH, RO_2, HO_2, and NO) are computed by QSSA relations,
- In the second procedure (b) two species (NO_2 and O_3) are added to the former QSSA species.

CONCLUSION

We have justified the use of lumping in air pollution modeling and we have proposed an algorithm for finding an appropriate lumping of species for any kinetic scheme. Such lumped species are necessary in order to apply reduction procedures. The application of such techniques to three distinct inorganic schemes has given good results in 1D cases including diffusion, emissions, and dry deposition. This validates the way we include a reduced kinetic scheme in a reaction-diffusion PDE [31]. The choice of a local algebraic constraint including only chemical production and loss gives good results and the accuracy remains below 1%. Using global algebraic constraints (chemical production and transport) does not seem to improve the accuracy, while computing the exact scheme at the boundary could induce improved results.

In contrast to previous works focused on numerical QSSA schemes [9, 24], such results indicate that reduced kinetic schemes give accurate results when they are used in an appropriate way.

We do not investigate in this article the CPU performance of reduced models. We focus only on the accuracy of such models and on some coupling strategies with diffusion and boundary conditions.

The extension to more complicated kinetic schemes in gas phase and in aqueous phase is a work in progress. Let us point out that the efficiency of such reduction procedures based on timescales is restricted by the number of fast timescales. An interesting approach is using a sensitivity analysis [10]. Another way we are currently investigating is the use of proper orthogonal decompositions (POD) [1].

APPENDIX A: KINETIC SCHEMES

The kinetic schemes are given in the Tables XV–XVII. The units have already been precised for each scheme. J stand for a photolytic kinetic rate.

TABLE XV
Kinetic Scheme for Ozone 16

No.	Reaction	Kinetic rate $a(b)$
1	$OD + AIR + O_2 \rightarrow O_3 + AIR + O_2$	6.02 (−34)
2	$O_3 + NO \rightarrow NO_2$	1.872 (−14)
3	$NO + HO_2 \rightarrow NO_2 + OH$	8.235 (−12)
4	$OH + NO_2 \rightarrow HNO_3$	1.1 (−11)
5	$NO_2 \rightarrow NO + OD$	8.88 (−3)
6	$RH + OH \rightarrow RO_2$	2.607 (−12)
7	$RCHO + OH \rightarrow RCO_3$	1.588 (−11)
8	$RCHO \rightarrow RO_2 + CO + HO_2$	3.18 (−6)
9	$NO + RO_2 \rightarrow RCHO + HO_2 + NO_2$	7.563 (−12)
10	$NO + RCO_3 \rightarrow NO_2 + RO_2 + CO_2$	7.563 (−12)
11	$NO_2 + RCO_3 \rightarrow PAN$	4.7 (−12)
12	$PAN \rightarrow RCO_3 + NO_2$	4.837 (−4)

Note. The kinetic rate is computed with $k = a10^b$.

The first reaction in Table XVII does not describe elementary processes and has been actually obtained by simplifying the mechanisms:

$$\begin{cases} O_3 + h\nu \xrightarrow{1a} O^* + O_2 \\ O^* + H_2O \xrightarrow{1b} 2OH \\ O^* + O_2 + M \xrightarrow{1c} O_3 + M \\ O^* + N_2 + O_2 \xrightarrow{1d} O_3 + N_2. \end{cases} \tag{A.1}$$

TABLE XVI
Kinetic Kim–Cho Scheme

No.	Reaction	Kinetic rate $a(b)$
1	$NO_2 \rightarrow NO + O_3$	9.6 (−3)
2	$O_3 + NO \rightarrow NO_2$	4.3 (−1)
3	$O_3 \rightarrow 2OH$	2.95 (−6)
4	$OH + NO \rightarrow HONO$	1.63 (2)
5	$OH + NO_2 \rightarrow HNO_3$	2.82 (2)
6	$HONO \rightarrow OH + NO$	2.8 (−3)
7	$HO_2 + NO \rightarrow NO_2 + OH$	2.07 (2)
8	$HO_2 + NO_2 \rightarrow HO_2NO_2$	2.82 (1)
9	$HO_2NO_2 \rightarrow HO_2 + NO_2$	8.48 (−2)
10	$HO_2 + HO_2 \rightarrow H_2O_2$	1.2 (2)
11	$H_2O_2 \rightarrow 2OH$	8.32 (−6)
12	$OH + CO \rightarrow HO_2 + CO$	7.28 (0)
13	$O_3 + NO_2 \rightarrow NO_3$	7.96 (−4)
14	$NO + NO_3 \rightarrow 2NO_2$	4.7 (−2)
15	$NO_2 + NO_3 \rightarrow N_2O_5$	4.35 (1)
16	$N_2O_5 \rightarrow NO_2 + NO_3$	7.4 (−2)
17	$N_2O_5 + H_2O \rightarrow 2HNO_3 + H_2O$	7.43 (−8)
18	$NO_3 \rightarrow 0.3NO + 0.7NO_2 + 0.7O_3$	1.49 (−1)
19	$OH + O_3 \rightarrow HO_2$	1.67 (0)
20	$HO_2 + O_3 \rightarrow OH$	3.84 (−2)
21	$OH + SO_2 \rightarrow H_2SO_4 + HO_2$	3.17 (1)

Note. The kinetic rate is computed with $k = a10^b$.

TABLE XVII
Kinetic Scheme Jacob

No.	Reaction	Kinetic rate $a(b)c$
1	$O_3 \rightarrow 2OH$	J
2	$OH + RH \rightarrow RO_2$	2.5 (−12) 0
3	$HO_2 + NO \rightarrow OH + NO_2$	3.7 (−12)−240
4	$OH + NO_2 \rightarrow HNO_3$	1.3 (−11) 0
5	$2HO_2 \rightarrow H_2O_2$	6.6 (−13)−620
6	$RO_2 + HO_2 \rightarrow ROOH$	4.1 (−13)−790
7	$RO_2 + NO \rightarrow NO_2 + HO_2$	4.2 (−12)−180
8	$NO_2 \rightarrow NO + O_3$	J
9	$NO + O_3 \rightarrow NO_2$	1.8 (−12) 1370

Note. The kinetic rate is computed with $k = a10^b \exp(\frac{-c}{T})$.

TABLE XVIII
Dry Deposition Velocity (cm s^{-1})

Species	O_3	NO_2	NO	H_2O_2	HNO_3
v_{Dep}	0.6	0.6	0.1	1	2.5

TABLE XIX
Emission Factors (molecules cm^{-3} s^{-1})

Species	q
RH	1.23E13
NO	0.7 × 2.52E12
NO_2	0.3 × 2.52E12

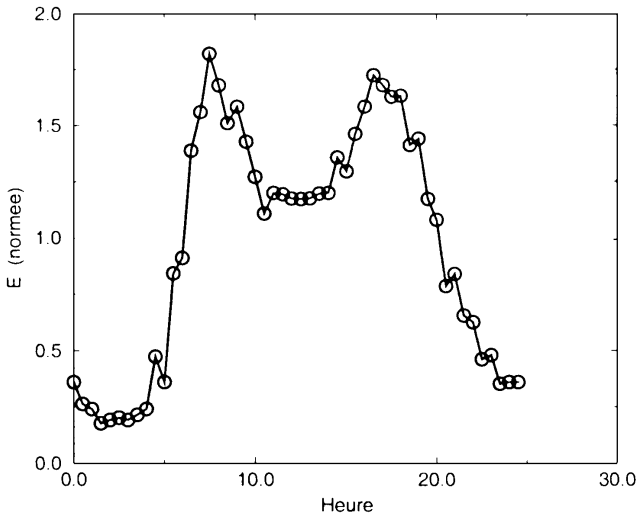

FIG. 3. Time evolution of E_w.

TABLE XX
Grid in the Monodimensional Case (m)

Cell	1	2	3	4	5	6	7	8	9	10	11
Δz	10	25	50	75	100	100	100	175	175	250	450

This leads to the photolytic rate:

$$J = J_{1a} \frac{k_{1b}\mathrm{H_2O}}{k_{1b}\mathrm{H_2O} + k_{1c}\mathrm{O_2} + k_{1d}\mathrm{N_2}}. \tag{A.2}$$

Reaction 8 is a photolytic reaction as well. The other kinetic rates are given by Arrhenius' law in the form

$$k(T) = aT^b \exp\left(-\frac{c}{T}\right), \tag{A.3}$$

where T is the temperature. We have used a constant temperature $T = 300$ K.

APPENDIX B: BOUNDARY CONDITIONS

The dry deposition velocity is given for some species in Table XVIII.

The emission rates are given as

$$E_i(t) = q_i E_w(t), \tag{B.1}$$

where $E_w(t)$ is plotted in Fig. 3. q_i is specific for each emitted species. Some values are given for the kinetic scheme Ozone 16 in Table XIX.

APPENDIX C: PARAMETERS FOR DIFFUSION

We have used a vertical grid determined by the meteorological solver. The length Δz is given in meters in Table XX.

The value of the turbulent diffusive coefficient is $k = 5\ \mathrm{m^2\ s^{-1}}$.

ACKNOWLEDGMENT

Part of this work was done in the framework of the A3UR project for the modeling of regional air pollution carried out at Electricité de France.

REFERENCES

1. G. Berkooz, P. Holmes, and J. L. Lumbey, The proper orthogonal decomposition in the analysis of turbulent flows, *Annu. Rev. Fluid Mech.*, 539 (1993).
2. E. Billette, *Etude mathématique de schémas de cinétique chimique: Application à des modèles de pollution.* Ph.D. thesis (Ecole Polytechnique, 1997).
3. W. P. L. Carter, A detailed mechanism for the gas-phase atmospheric reactions of organic compounds. *Atmos. Environ.* **24**, 481 (1990).

4. M. Coderch, A Willsky, S. S. Sastry, and D. A. Castanon, Hierarchical aggregation of linear systems with multiple time scales, *IEEE Trans. Autom. Control* **AC 28**(11) (1983).
5. P. Deuflhard, Recent progress in extrapolation methods for ode's, *SIAM Review* **27**, 505 (1985).
6. P. Deuflhard, E. Hairer, and J. Zugck, One step and extrapolation method for differential-algebraic systems, *Num. Math.* **51**, 501 (1987).
7. R. Djouad and B. Sportisse, Solving differential-algebraic reduced systems arising in air pollution modelling (2000), submitted.
8. P. Duchêne and P. Rouchon, Kinetic scheme reduction via geometric singular perturbation techniques, *Chem. Eng. Sci.* **51**(20) (1996).
9. Gong and Cho, A numerical scheme for the integration of the gas-phase chemical rate equations in 3d atmospheric models. *Atmos. Environ.* **27A**, 2591 (1993).
10. A. C. Heard, M. J. Pilling, and A. S. Tomlin, Mechanism reduction techniques applied to tropospheric chemistry, *Atmos. Environ.* **32**(6), 1059 (1998).
11. O. Hertel, R. Berkowicz, and J. Christensen, Test of two numerical schemes for use in atmospheric transport-chemistry models, *Atmos. Environ.* **27A**(16), 2591 (1993).
12. E. Hesstvedt, O. Hov, and I. S. A. Isaksen, Qssas in air polution modelling: Comparison of two numerical schemes for oxydant prediction, *Int. J. Chem. Kinet.* **10**, 971 (1978).
13. A. C. Hindmarsh, *Scientific Computing, Chapter ODEPACK: A Systematized Collection of ODE Solvers* (North Holland, 1983).
14. J. Kim and S. Y. Cho, Computation accuracy and efficiency of the time-splitting method in solving atmospheric transport-chemistry equations, *Atmos. Environ.* **31**(15), 2215 (1997).
15. S. H. Lam, *Reduced Chemistry Modelling and Sensitivity Analysis*, Lectures notes for aerothermochemistry for hypersonic technology (Von Karman Institute, 1995).
16. S. H. Lam and D. A. Goussis, Understanding complex chemical kinetics with computational singular perturbation, in *Twenty-Second Symposium on Combustion* (1988).
17. S. H. Lam and D. A. Goussis, The csp method for simplifying kinetics, *Int. J. Chem. Kinet.* **26** (1994).
18. G. Li, A lumping analysis in mono and bimolecular reaction systems, *Chem. Eng. Sci.* **29**(7–8), 1261 (1984).
19. G. Li and H. Rabitz, A general analysis of exact lumping in chemical kinetics, *Chem. Eng. Sci.* **44**(6), 1413 (1989).
20. G. Li, A. S. Tomlin, H. Rabitz, and J. Toth, Determination of approximate lumping schemes by a singular perturbation method, *J. Chem. Phys.* **99**(5) (1993).
21. R. M. Lowe and A. S. Tomlin, The application of repro-modeling to a tropospheric chemistry model, in *Proceedings APMS'98* (ENPC-INRIA, 1998), p. 423.
22. U. Maas and S. B. Pope, Simplifying chemical kinetics: Intrinsic low-dimensional manifolds in composition space, *Combust. Flame* **88**, 239 (1992).
23. P. A. Makar and S. M. Polaravapu, Analytic solutions for gas-phase chemical mechanism compression, *Atmos. Environ.* **31**(7), 1025 (1997).
24. R. Mathur, J. O. Young, K. L. Schere, and G. L. Gipson, A comparison of numerical techniques for solution of atmospheric kinetic equations, *Atmos. Environ.* **32**(9), 1535 (1998).
25. G. J. McRae, W. R. Goodin, and J. H. Seinfeld, Numerical solution of the atmospheric diffusion equation for chemically reacting flows, *J. Comput. Phys.* **45**, 1 (1982).
26. L. R. Petzold and W. Zhu, Model reduction for chemical kinetics: An optimization approach, Technical Report MN 55455, Dept. of Computer Science, Un. Minnesota (1997).
27. A. Sandu, J. G. Verwer, M. Van Loon, G. Carmichael, F. A. Potra, D. Dabdub, and J. H. Seinfeld, Benchmarking stiff odes solvers for atmospheric chemistry problems i: Implicit versus explicit, *Atmos. Environ.* **31**, 3151 (1997).
28. J. H. Seinfeld, *Atmospheric Physics and Chemistry of Air Pollution* (Wiley, 1985).
29. B. Sportisse, *Contribution à la modélisation des écoulements réactifs: réduction des modèles de cinétique chimique et simulation de la pollution atmosphérique*, Ph.D. thesis (Ecole Polytechnique, 1999).

30. B. Sportisse, An analysis of operator splitting techniques in the stiff case, *J. Comput. Phys.* **161**, 140 (2000).
31. B. Sportisse and P. Rouchon, Reduction of slow-fast chemistry with slow processes. Technical Report 98-129, CERMICS (1999).
32. Pu Sun, D. Chock, and S. L. Winkler, An implicit-explicit hybrid solver for a system of stiff kinetic equations, *J. Comput. Phys.* **115**, 515 (1994).
33. A. N. Tikhonov, A. B. Vasileva, and A. G. Sveshnikov, *Differential Equations* (Springer–Verlag, 1985).
34. A. S. Tomlin, G. Li, H. Rabitz, and J. Toch, A general analysis of approximate nonlinear lumping in chemical kinetics. ii constrained lumping, *J. Chem. Phys.* **101**(2) (1994).
35. T. Turanyi, A. S. Tomlin, and M. J. Pilling, On the error of the quasi-steady state approximation, *J. Phys. Chem.* **97**, 163 (1993).
36. V. Van Breusegem and G. Bastin, A singular perturbation approach to the reduced order dynamical modelling of reaction systems, Technical report, Université catholique de Louvain Belgique (1993).
37. J. G. Verwer, J. Blom, M. Van Loon, and E. J. Spee, A comparison of stiff odes solvers for atmospheric chemistry problems, *Atmos. Environ.* **30**, 49 (1996).
38. J. G. Verwer, W. H. Hundsdorfer, and J. G. Blom, Numerical time integration for air pollution models, in *Proceedings of the Conference APMS'98* (ENPC-INRIA, 1998).
39. A. I. Vol'pert and S. I. Hudjaev, *Analysis in Classes of Discontinuous Functions and Equations of Mathematical Physics*, chapter 12 (Martinus Nijhoff, 1985).
40. J. Wei and J. C. W. Kuo, A lumping analysis in monomolecular reaction systems: Analysis of approximately lumpable system, *IEC Fundam.* **8**(1) (1969).
41. J. Wei and J. C. W. Kuo, A lumping analysis in monomolecular reaction systems: Analysis of the exactly lumpable system, *IEC Fundam.* **8**(1) (1969).
42. J. H. Wilkinson, *The Algebraic Eigenvalue Problem* (Oxford Science Publication, 1992).
43. T. R. Young and J. P. Boris, A numerical technique for solving stiff ode associated with the chemical kinetics of reaction flow problems, *J. Phys. Chem.* **81**, 2424 (1977).
44. Z. Zlatev, *Computer Treatment of Large Air Pollution Models* (Kluwer, 1995).